Sensitivity of Net Radiation to Snow in a Canadian Rocky Mountain Basin

C.R. Ellis* and J.W. Pomeroy

Centre for Hydrology, University of Saskatchewan, 117 Science Place, Saskatoon, Saskatchewan, Canada, S7N 5C8

***e-mail: cre152@mail.usask.ca**

Introduction

Radiation is the dominant energy source for snowmelt. Net radiation to snow (R^*) is made up of net shortwave (K^*) and net longwave (L^*) radiation, each composed of incoming and outgoing fluxes, i.e.

$$R^* = K^* + L^* = K_{in} - K_{out} + L_{in} - L_{out}$$

Forest cover strongly controls radiation to snow by absorption and reflection of shortwave radiation while increasing longwave radiation via forest thermal emissions. The cumulative effect of forest cover on radiation is strongly dependent on meteorology, which in mountain regions is further complicated by topographical effects on shortwave irradiance. As such, changes in forest cover density are expected to have different effects on forest radiation and snowmelt for varying slopes and aspects.

Objective

The objective of this study is to investigate how forest cover density controls net radiation to forest snow with varying topography. This will be accomplished through simulations using a physically-based model describing forest radiation transfers with varying slope and aspect, as well as longwave exitance (L_{out}) from snow.

Model Description

Estimation of shortwave irradiance to snow (K_{in}):

Forest cover density may be expressed by the sky view factor, v, defined as the fraction of the overlying sky hemisphere not occupied by forest. More formally, v may be defined over the hemisphere by :

$$v = 2\int_0^{\pi/2} e^{-\frac{L`\xi}{\sin\theta}} \sin\theta\cos\theta \cdot d\theta$$

where θ is the elevation angle above the local horizon [radians], ξ is the dimensionless vertical forest depth, and $L`$ is the leaf area index effective for radiation transfer (i.e. account is made for foliage clumping and the vertical leaf inclination distribution is assumed spherical). For conditions of isotropic shortwave irradiance throughout the sky, forest shortwave transmittance (τ) equals v. However, under more typical conditions where a disproportionate amount of direct beam radiation is received from the position of the sun, τ is determined as:

$$\tau = e^{-L`\xi_{eff}}$$

where ξ_{eff} is the effective forest shortwave extinction depth, which is calculated as the weighted sum of diffuse and direct beam depths, i.e.

$$\xi_{eff} = (1-k_d)\xi_b + k_d\left(-\frac{\ln(v)}{L`}\right)$$

Here, k_b and k_d are the respective direct beam and diffuse shortwave fractions, and ξ_b is the forest depth for direct beam irradiance transfer, which is determined via spherical geometry for beam irradiance received from a solar position of θ elevation and φ azimuth by:

$$\xi_b(\theta,\varphi) = \frac{\xi\cos(\theta_s)}{\sin(\theta_s)\cos(X(\theta,\varphi)\text{^}S(\theta,\varphi))}$$

where θ_s is the solar elevation above the horizon, and X and S are the respective slope gradient and azimuth of level and sloped surfaces. Net shortwave radiation (K^*), with account for shortwave enhancement to snow via forest-snow multiple reflections is determined by:

$$K^* = \frac{K_o\tau(1-\alpha_s)}{1-\alpha_s\alpha_c(1-v)}$$

where K_o is the above-canopy irradiance, α_s is the snow albedo, and α_c is the forest albedo.

Estimation of longwave irradiance to snow (L_{in}):

Longwave irradiance (L_{in}) to forest snow is estimated as the sum of sky longwave irradiance (L_o) and forest longwave emissions, weighed by v, i.e.

$$L_{in} = vL_o + (1-v)\varepsilon\sigma T_f^4$$

where ε is the forest emissivity [ ], σ is the Stephan-Boltzmann constant [5.67 x 10^{-8} W m^{-2} K^{-4}], and T_f is the effective forest temperature [K]. Often, T_f is approximated by air temperature, which may lead to substantial underestimation of T_f and L_{in} especially in forests heated by shortwave absorption. Alternatively, T_f is estimated first by resolving the energy content of the forest's wood component (i.e. non-green foliage) (dU/dt) [W m^{-2}]:

$$dU/dt = J^*_K + J^*_L + J^*_H + J^*_E + J^*_W$$

where J^*_K and J^*_L are the respective net forest shortwave and longwave radiations, J^*_H is the net sensible heat transfer, J^*_E is latent heat transfer due to phase change and J^*_W the net heat conductive transfer between the outer and inner biomass layers of the forest. However, due to the strong absorption of longwave radiation by forest material, not all longwave emissions from heated foliage are received at the sub-canopy. The total probability of longwave emissions from heated foliage being received at the sub-canopy (P_h) from a fraction of the dimensionless forest depth (d/ξ) is given by the joint probabilities of shortwave absorption (P_a) and longwave transmission to the sub-canopy (P_r) (Figure 1), which may be approximated by $L`$ by:

$$P_{h(d/\xi)} = e^{-L`\xi_{eff}\,d/\xi}\cdot e^{-L`(1-d/\xi)} = e^{-(L`+(\xi_{eff}L`-L`)d/\xi)}$$

and integrated over the entire vertical forest profile via:

$$P_{h(0\to\xi)} = \int_0^{\xi} e^{-(L`+(L`\xi_{eff}-L`)d/\xi)}\,d\,d/\xi \cong \frac{e^{-L`}(1-e^{-(L`\xi_{eff}-L`)})}{L`\xi_{eff}-L`}$$

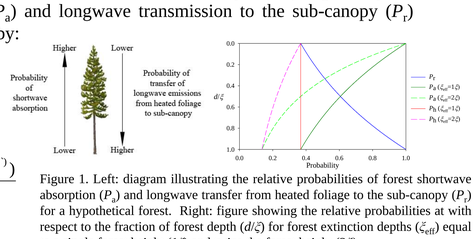

Figure 1. Left: diagram illustrating the relative probabilities of forest shortwave absorption (P_a) and longwave transfer from heated foliage to the sub-canopy (P_r) for a hypothetical forest. Right: figure showing the relative probabilities at with respect to the fraction of forest depth (d/ξ) for forest extinction depths (ξ_{eff}) equal to a single forest height (1ξ) and twice the forest height (2ξ).

Estimation of longwave exitance from snow (L_{out}):

A critical radiation term is the longwave exitance from snow (L_{out}), which is directly related to the snow surface temperature, T_s. Ventilation of the snow surface depresses its temperature to a balance between the net longwave radiation and the ice-bulb temperature, which is calculated using the following longwave-psychrometric expression by Pomeroy *et al*. (in preparation):

$$T_s = T_a + \frac{\varepsilon\left(L_{in} - \sigma T_a^4\right) + \lambda_v\left[Q_a - Q_{sat}(T_a, P_s)\right]\rho/r_a}{\varepsilon\sigma T_a^3 + (c_p + \lambda_v\Delta)\rho/r_a}$$

where λ_v is the latent heat of vapourization [J kg^{-1}], Q_a and Q_{sat} are the observed and saturation vapour pressures of air, r_a is the aerodynamic resistance, ρ is the density of air, c_p is the heat capacity of air and Δ is the slope of the Clausius-Clapeyron equation relating Q_{sat} to air temperature (T_a).

Model evaluation:

Meteorological data for model evaluation and forcing were obtained from forest and open sites of varying topography and elevation within the Marmot Creek Research Basin (MCRB), located in the Kananaskis River valley, Alberta (Figure 2).

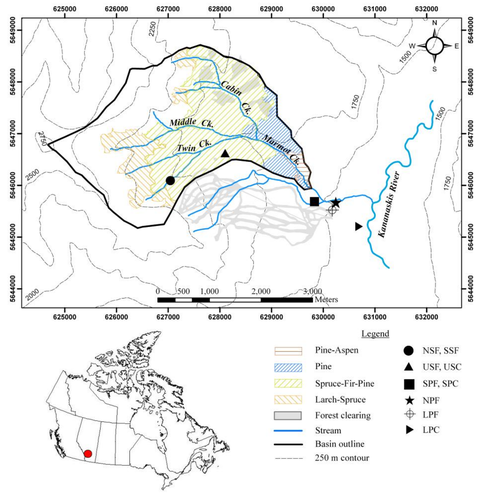

Figure 2. Map of the Marmot Creek Research Basin (MCRB) showing the meteorological stations of the study, main stream network, and primary forest cover types.

Simulations of sub-canopy shortwave and longwave were made for lodgepole pine forests on level (LPF), southeast-sloping (SPF) and north-sloping (NPF) topography. Forest cover parameters for the simulations were acquired by analysis of forest hemispherical images. Results show the model is able to well represent the substantial differences in sub-canopy shortwave and longwave irradiance (Figure 3). Simulations of sub-canopy longwave irradiance using the forest energy-balance model reduced the underestimation using air temperature from 4% to 1%.

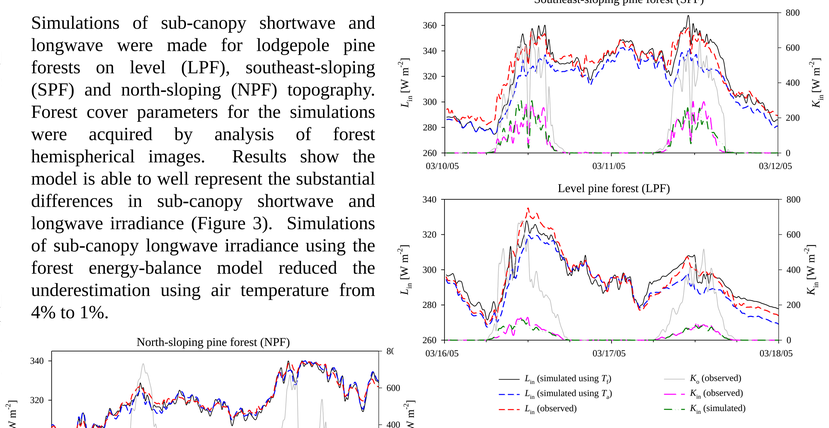

Figure 3. Comparison of simulated and observed shortwave (K_{in}) and longwave irradiance (L_{in}) at a southeast-sloping pine forest (top), level pine forest (above) and a north-sloping pine forest (left). K_o is the observed shortwave irradiance to a level pine clearing (LPC)

Simulations of snow surface temperature (T_s) show the longwave-psychrometric model provides good comparison to observed temperatures at the south-sloping spruce forest (SSF). Here, mean observed and simulated T_s equaled -9.1°C and -8.7, respectively, compared to mean air temperature (T_a) of -7.7° C.

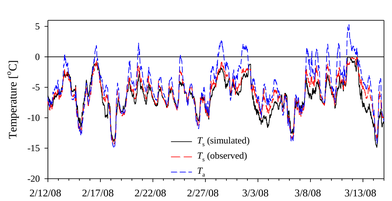

Figure 4. Time series of air temperature (T_a), as well as simulated and observed snow surface temperature (T_s) at the south-sloping spruce forest site (SSF).

Model Application

Simulations of net radiation (R^*) were performed for sites of 30° south-sloping, level, and 30° north-sloping topography. Model forcing data was provided from observations of radiation in a level pine clearing (LPC), as well pine forest meteorological observations. Simulations were performed for two snow albedo (α_s) conditions: a relatively high snow albedo (α_s=0.8) and a relatively low snow albedo (α_s=0.7). To assess the potential effects of forest cover on mountain snowmelt, simulations were conducted for the period extending from February to June. Meteorological conditions during the period are shown in Fig. 5.

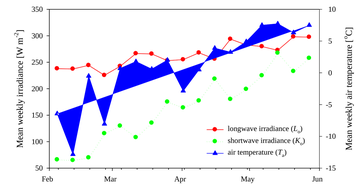

Figure 5. Mean weekly shortwave irradiance (K_o), longwave irradiance (*Lo*), and air temperature observed at the LPC.

To illustrate the effect of forest cover density on radiation, the sky view factor (v) at which maximum simulated net radiation (R^*) to snow occurs for all three sites is shown in Figure 6. Here, for all sites in early February, maximum R^* is realized for at low v, when longwave radiation gains from higher canopy closure more than offset any reductions in shortwave irradiance. However, as shortwave irradiance increases through the spring, maximum R^* occurs for higher v, starting with the south-sloping site where shortwave receipts are greatest. By contrast, due to low shortwave irradiance to the north-sloping site, maximum R^* continues to occur at very low v until mid-May. Note that even at the end of May, when shortwave irradiance is greatest, maximum R^* at the north-sloping site is received at a v substantially less than 1 for the condition of high α_s. Figure 7 shows that regardless of α_s, maximum R^* is very similar among sites during mid-winter, with increasing divergence through spring, with the greatest and least R^* at the south-sloping and north-sloping sites, respectively.

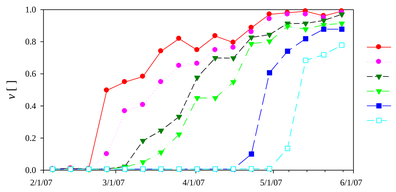

Figure 6. Sky view factor (v) at which maximum net radiation to snow (R^*) (weekly average) occurs for snow albedo (α_s) equal to 0.8 and 0.7 at south-sloping, level, and north-sloping sites.

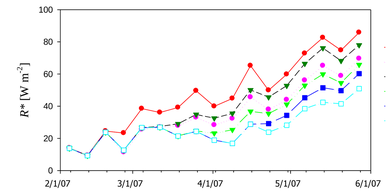

Figure 7. Maximum (weekly average) radiation to snow (R^*) for snow albedo (α_s) of 0.8 and 0.7 at south-sloping, level, and north-sloping sites.

The effect of forest cover on radiation is further illustrated in Figure 8, which shows R^* at a v of 0 (i.e. complete canopy closure and therefore R^* does not vary with topography) and v of 1 (i.e. no forest cover) for the two snow albedo conditions (α_s). For both α_s, greater R^* occurs nearly always under forest cover at all sites during mid to late winter. However, in the spring, greater R^* is received in the open at the south-sloping and level sites from increased shortwave gains. By contrast, greater R^* at the north-sloping site is almost always realized under forest cover throughout winter and spring. The strong effect of α_s on R^* is seen especially at the south-sloping and level sites, where the lowering of α_s from 0.8 to 0.7 results in R^* in the open exceeding that in the forest occurring nearly a month earlier. Alternatively, R^* at the north-sloping site is much less sensitive to α_s, resulting in higher R^* occurring nearly always under forest cover, as the strongly negative longwave balance offsets the modest shortwave gains to the open site.

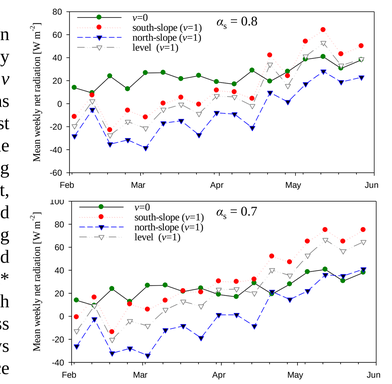

Figure 8. Net radiation to snow (R^*) under complete forest cover (i.e. v=0) and in the open (i.e. v=1) at south-sloping, level, and north-sloping sites for snow albedo (α_s) of 0.8 (top) and 0.7 (bottom).

Conclusions

Results from the above simulations reveal that topography exerts a strong control on how changes in needleleaf forest cover affect net radiation to mountain snowcover. However, the direction and magnitude of these effects vary temporally over the late winter-spring period due to seasonal changes in shortwave irradiance and air temperature. During the late winter, low shortwave irradiance results in a small variation of radiation to snow between sites of differing topography; greater radiation occurs with increased forest density due to the additional longwave irradiance from forest emissions. However, as shortwave irradiance increases through the spring, greater radiation to snow occurs at low forest densities, starting with the south-sloping and level sites. By contrast, higher radiation is received under forest cover relative to open snow at north-sloping sites due to the additional forest longwave emissions more than compensating for reductions in shortwave radiation. This suggests that the timing and rate of snowmelt on south-sloping and level sites will react very differently from north-sloping sites to changes in needleleaf forest cover density, with forest removal advancing melt at the former sites while delaying melt in the latter. This result may explain some of the ambiguous experimental basin results on the effect of forest removal on snowmelt rates.

Acknowledgements

The authors thank Mr. Tom Brown (Centre for Hydrology) for model incorporation into the Cold Regions Hydrological Model (CRHM) platform. Support for this study was provided for by the Natural Science and Engineering Council of Canada (NSERC) CGS-D (Ellis) and by the IP3 Network funded by the Canadian Foundation for Climate and Atmospheric Sciences (CFCAS).